

RIPK1-dependent apoptosis bypasses pathogen blockade of innate signaling to promote immune defense

Lance W. Peterson,^{1,2} Naomi H. Philip,^{1,2} Alexandra DeLaney,^{1,2} Meghan A. Wynosky-Dolfi,^{1,2} Kendra Asklof,¹ Falon Gray,¹ Ruth Choa,^{1,2} Elisabet Bjanas,^{1,2} Elisabeth L. Buza,¹ Baofeng Hu,^{1,2} Christopher P. Dillon,³ Douglas R. Green,³ Scott B. Berger,⁴ Peter J. Gough,⁴ John Bertin,⁵ and Igor E. Brodsky^{1,2}

¹Department of Pathobiology, University of Pennsylvania School of Veterinary Medicine, Philadelphia, PA

²Institute for Immunology, University of Pennsylvania Perelman School of Medicine, Philadelphia, PA

³Department of Immunology, St. Jude Children's Research Hospital, Memphis, TN

⁴Host Defense Discovery Performance Unit, Infectious Disease Therapy Area Unit and ⁵Pattern Recognition Receptor Discovery Performance Unit, Immunology Inflammation Therapeutic Area, GlaxoSmithKline, Collegeville, PA

Many pathogens deliver virulence factors or effectors into host cells in order to evade host defenses and establish infection. Although such effector proteins disrupt critical cellular signaling pathways, they also trigger specific antipathogen responses, a process termed "effector-triggered immunity." The Gram-negative bacterial pathogen *Yersinia* inactivates critical proteins of the NF- κ B and MAPK signaling cascade, thereby blocking inflammatory cytokine production but also inducing apoptosis. *Yersinia*-induced apoptosis requires the kinase activity of receptor-interacting protein kinase 1 (RIPK1), a key regulator of cell death, NF- κ B, and MAPK signaling. Through the targeted disruption of RIPK1 kinase activity, which selectively disrupts RIPK1-dependent cell death, we now reveal that *Yersinia*-induced apoptosis is critical for host survival, containment of bacteria in granulomas, and control of bacterial burdens in vivo. We demonstrate that this apoptotic response provides a cell-extrinsic signal that promotes optimal innate immune cytokine production and antibacterial defense, demonstrating a novel role for RIPK1 kinase-induced apoptosis in mediating effector-triggered immunity to circumvent pathogen inhibition of immune signaling.

INTRODUCTION

Innate immune cells mount protective responses against pathogens through the recognition of conserved microbial structures known as pathogen-associated molecular patterns (PAMPs; Janeway, 1989). However, pathogens use virulence mechanisms, including injection of specialized proteins known as effectors, to interfere with cellular physiology and evade recognition by the host immune system (Brodsky and Medzhitov, 2009; Reddick and Alto, 2014). Furthermore, PAMPs are highly conserved across microbial classes and are present in both harmless or beneficial commensals and potentially dangerous pathogens. Generating appropriate responses to pathogens therefore relies on the sensing of pathogen-specific activities or "patterns of pathogenesis" (Vance et al., 2009). This mechanism of recognizing pathogens by their effector activities has also been termed "effector-triggered immunity" and, like PAMP recognition, is evolutionarily conserved in multicellular eukaryotes (Stuart et al., 2013). However, in the case of mammals, the mechanisms by which

effector-triggered immunity promotes host defense remain poorly understood (Stuart et al., 2013).

Induction of regulated cell death is a central feature of infection by many pathogens. Although necrotic cell death and caspase-1- or caspase-11-dependent pyroptotic cell death are well-established mediators of inflammatory responses, apoptosis is generally viewed as a quiescent or immunosuppressive form of cell death (Green et al., 2009; Galluzzi et al., 2017). However, apoptosis can also act as an immunogenic stimulus to induce adaptive immune responses under specific circumstances (Galluzzi et al., 2017). This includes the induction of adaptive T_H1 and T_H17 responses in the context of treatment with chemotherapeutic agents or during phagocytosis of apoptotic cells containing bacterial products (Nowak et al., 2003; Casares et al., 2005; Torchinsky et al., 2010; Campisi et al., 2016; Galluzzi et al., 2017). This suggests that apoptosis occurring in the context of infection by bacterial pathogens might also facilitate induction of innate immune responses through poorly defined signaling pathways.

Yersinia species are extracellular Gram-negative bacterial pathogens that can cause disease in humans and animals,

Correspondence to Igor E. Brodsky: ibrodsky@vet.upenn.edu

N.H. Philip's present address is Dept. of Immunobiology, Yale University School of Medicine, New Haven, CT.

Abbreviations used: LDH, lactate dehydrogenase; MLN, mesenteric LN; PAMP, pathogen-associated molecular pattern; TC, tissue culture; TNFR, TNF receptor; *Yp*, *Yersinia pseudotuberculosis*.

© 2017 Peterson et al. This article is distributed under the terms of an Attribution-Noncommercial-Share Alike-No Mirror Sites license for the first six months after the publication date (see <http://www.rupress.org/terms/>). After six months it is available under a Creative Commons License (Attribution-Noncommercial-Share Alike 4.0 International license, as described at <https://creativecommons.org/licenses/by-nc-sa/4.0/>).



ranging from plague to gastroenteritis and mesenteric lymphadenitis. *Yersinia* species use effector proteins that are injected into a target cell to inhibit signaling pathways and establish disease (Viboud and Bliska, 2005). One such effector protein is an acyltransferase known as YopJ, which is a member of a family of evolutionarily conserved effector proteins in pathogens of eukaryotic organisms (Orth et al., 2000; Mukherjee et al., 2007; Cheong et al., 2014). YopJ inhibits TAK1, IKK, and MKK proteins that are key activators of NF- κ B and MAPK pathways downstream of TLRs, leading to blockade of inflammatory cytokine production by *Yersinia*-infected cells (Boland and Cornelis, 1998; Ruckdeschel et al., 1998; Palmer et al., 1999; Zhang et al., 2005; Mittal et al., 2006; Mukherjee et al., 2006; Paquette et al., 2012). Importantly, this activity of YopJ triggers cell death via caspase-8-dependent apoptosis that also engages caspase-1 (Philip et al., 2014; Weng et al., 2014), raising the possibility that YopJ-induced cell death represents an effector-triggered immune response.

We recently found that *Yersinia*-induced cell death requires combined activity of both TLR4/TRIF and TNF receptor 1 (TNFR1) signaling, which together activate caspase-8 and caspase-1 through the kinase activity of receptor-interacting protein kinase 1 (RIPK1; Peterson et al., 2016). Interestingly, RIPK1 is a central control point for induction of both cell death and cytokine gene expression in response to inflammatory stimuli (Ofengeim and Yuan, 2013). Ubiquitination of RIPK1 promotes assembly of an NF- κ B- and MAPK-activating complex (known as complex I) downstream of TNFR1 or TLRs (Hsu et al., 1996; Kelliher et al., 1998; Meylan et al., 2004; Cusson-Hermance et al., 2005; Ofengeim and Yuan, 2013). Assembly of this signaling complex generally does not require RIPK1 kinase activity (Hsu et al., 1996; Ting et al., 1996; Lee et al., 2004; Berger et al., 2014; Newton et al., 2014). Alternatively, RIPK1 kinase activity promotes extrinsic apoptosis or programmed necrosis through specific interactions with caspase-8 or RIPK3, respectively, within complex II (Grimm et al., 1996; Hsu et al., 1996; Ting et al., 1996; Kelliher et al., 1998; Holler et al., 2000; Micheau and Tschopp, 2003; Degterev et al., 2008). Specific disruption of RIPK1 kinase activity, therefore, blocks cell death independently of cytokine production (Berger et al., 2014; Newton et al., 2014; Philip et al., 2014).

The contribution of RIPK1 kinase-dependent cell death to inflammatory responses has been primarily attributed to its role in RIPK3-dependent necroptosis (Berger et al., 2014; Newton et al., 2014, 2016; Polykratis et al., 2014; Silke et al., 2015; Weinlich et al., 2017). Although a recent study has suggested a necroptosis-independent function for RIPK1 kinase activity in regulating pathological inflammation (Newton et al., 2016), whether RIPK1-induced apoptosis plays a direct role in host defense has not been examined. Interestingly, pharmacological blockade of TAK1 leads to RIPK1 kinase-dependent apoptosis (Dondelinger et al., 2013, 2015; Ting and Bertrand, 2016; Jaco et al., 2017), but a physiological role for this response has not yet been described.

Here, we demonstrate that mice specifically lacking RIPK1 kinase activity have a defect in *Yersinia*-induced apoptosis in vivo, fail to control systemic bacterial burdens, and succumb rapidly to infection. Surprisingly, RIPK1 kinase activity was required for optimal inflammatory cytokine production by inflammatory monocytes and neutrophils. This response was RIPK3-independent and required cell-extrinsic RIPK1 kinase activity, suggesting that RIPK1-induced apoptosis is associated with the release of inflammatory signals in vivo. The susceptibility of RIPK1 kinase-deficient animals was ameliorated during infection with YopJ-deficient bacteria, indicating that RIPK1 is a key regulator of effector-triggered immunity that responds to blockade of NF- κ B and MAPK signaling by the bacterial effector YopJ. Together, these data provide the first direct demonstration that RIPK1 kinase-dependent apoptosis promotes inflammatory responses against pathogens and shed new light on the role of RIPK1 in immune defense.

RESULTS AND DISCUSSION

RIPK1 kinase activity is required for *Yersinia*-induced apoptosis

Yersinia pseudotuberculosis (*Yp*) infection induces apoptosis of innate immune cells both in vitro and in vivo through the activity of the virulence factor YopJ (Monack et al., 1997, 1998; Ruckdeschel et al., 1998). This cell death is triggered by TLR4/TRIF and TNFR1 signaling, which together activate extrinsic apoptosis through caspase-8 and RIPK1 kinase activity (Haase et al., 2003; Zhang and Bliska, 2003; Ruckdeschel et al., 2004; Gröbner et al., 2007; Philip et al., 2014; Weng et al., 2014; Peterson et al., 2016). Importantly, we observed that BMDMs from RIPK1 “kinase-dead” mice (*Ripk1^{kd}*), which have genetically ablated RIPK1 kinase activity (Berger et al., 2014), showed loss of YopJ-induced cell death equivalent to that of BMDMs treated with a specific inhibitor of RIPK1 kinase activity, necrostatin-1 (Nec-1; Fig. 1 A). Notably, genetic ablation of RIPK1 kinase activity also abrogated YopJ-induced cleavage of caspase-8 and caspase-3 (Fig. 1, B and C).

In the absence of caspase inhibition, RIPK1 kinase activity is dispensable for cytokine production in response to direct TLR and TNFR stimulation (Ting et al., 1996; Lee et al., 2004; Berger et al., 2014; Newton et al., 2014; Philip et al., 2014; Najjar et al., 2016). Consistently, inflammatory cytokine production by *Ripk1^{kd}* BMDMs was indistinguishable from that of WT BMDMs in response to YopJ-deficient *Yersinia* (Δ YopJ) or TLR ligand treatment (Fig. 1, D and E). As expected, BMDMs infected with WT *Yp* produced dramatically less TNF because of YopJ-dependent inhibition of cell signaling, but there was no difference in TNF production between WT and *Ripk1^{kd}* cells (Fig. 1 D).

Although BMDMs undergo apoptosis in response to *Yersinia* infection in vitro, specific cell populations that undergo RIPK1 kinase-dependent apoptosis during in vivo *Yersinia* infection have not been investigated. Staining for

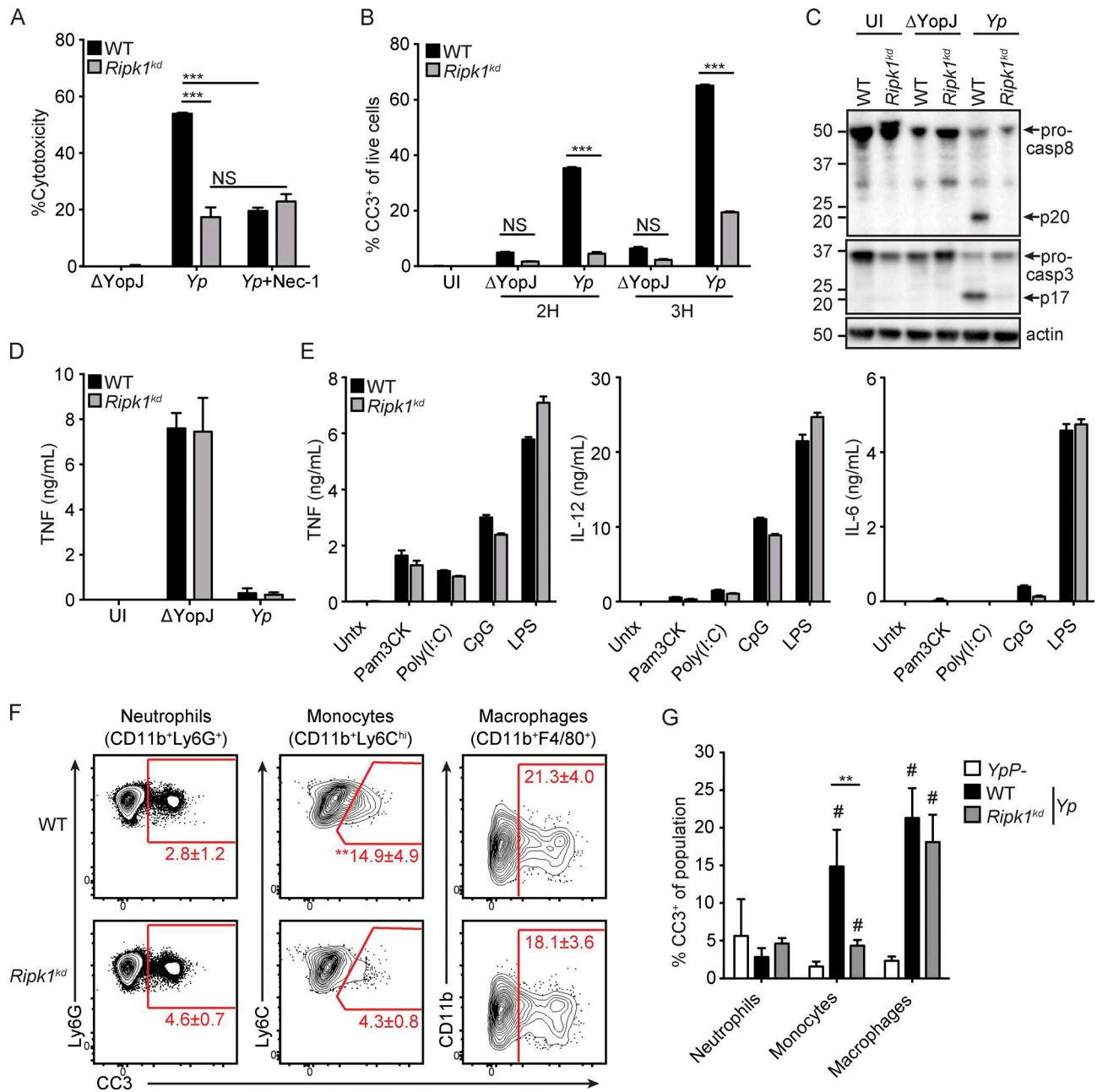


Figure 1. RIPK1 kinase activity is required for *Yersinia*-induced apoptosis. WT and *Ripk1^{kd}* BMDMs were treated with 60 μ M of the RIPK1 inhibitor Nec-1 or control media and infected with YopJ-deficient (Δ YopJ) or WT (Yp) *Y. pseudotuberculosis*. (A) Cell death was measured by LDH release assay at 4 h postinfection. (B and C) Apoptotic caspase cleavage was assessed by flow cytometry staining for CC3 (B) and Western blotting of lysates (C) 2 h postinfection. Molecular mass is indicated in kilodaltons. (D and E) Supernatants of BMDMs were measured for release of TNF at 4 h postinfection (D) or for TNF, IL-12p40, and IL-6 at 6 h after treatment with TLR ligands (E). Data are representative of more than three independent experiments in A and two independent experiments in B–E. Graphs show mean and SD of triplicate experiments. (F) Splenocytes were harvested 4 h after intravenous infection with Yp and stained for the indicated cell types and CC3. (G) Percentage of WT and *Ripk1^{kd}* CC3⁺ spleen cells infected with Yp relative to WT mice infected with the virulence plasmid-deficient strain (YpP⁻). Flow cytometry numbers and bar graph show mean and SD ($n = 4$ –5 mice per group) values representative of two independent experiments. #, $P < 0.05$ compared with YpP⁻ infection. Statistical differences were determined by Student's t test. **, $P < 0.01$; ***, $P < 0.001$; NS, not significant.

cleaved caspase-3 (CC3) after intravenous *Yp* injection revealed that splenic Ly6C^{hi} monocytes and F4/80⁺ macrophages, but not neutrophils, undergo rapid apoptosis after injection of WT, but not an isogenic avirulent *Yersinia* strain that lacks the virulence plasmid (*YpP*). Interestingly, in vivo apoptosis of monocytes, but not macrophages, was significantly reduced in *Ripk1^{kd}* mice, suggesting a cell type-specific role for RIPK1 kinase activity in vivo (Fig. 1, F and G). Together, these data demonstrate that targeted genetic disruption of RIPK1 kinase activity blocks *Yersinia*-induced apoptosis without influencing cell-intrinsic cytokine production, allowing us to specifically dissect the role of in vivo pathogen-induced apoptosis in host defense.

RIPK1 kinase activity protects against in vivo *Yersinia* infection

Strikingly, *Ripk1^{kd}* mice exhibited 100% mortality within 10 d after oral infection with *Yp* under conditions in which WT mice almost uniformly survive (Fig. 2 A; Zhang and Bliska, 2010; Fonseca et al., 2015). At day 5 postinfection, *Ripk1^{kd}* mice had significantly increased bacterial burdens in spleen and liver, but not in mesenteric LNs (MLNs; Fig. 2 B). *Ripk1^{kd}* animals also had significant bacterial burdens in their lungs, whereas the majority of WT animals had undetectable bacterial burdens in this tissue (Fig. 2 C). These data suggest that RIPK1 kinase activity is critical for limiting dissemination, replication, or clearance of *Yp* in systemic tissues. Interestingly, splenic bacterial burdens between WT and *Ripk1^{kd}* mice were equivalent after intraperitoneal infection (Fig. S1 A), suggesting that RIPK1 kinase activity regulates *Yp* infection in an organ- and route-dependent manner. RIPK1 kinase-dependent responses occurring at the level of the intestine or MLN may therefore limit dissemination to systemic tissues. Notably, acute blockade of RIPK1 by oral treatment of WT mice with a novel pharmacologic inhibitor of RIPK1 kinase activity (unpublished data) also significantly reduced resistance to oral *Yp* infection (Fig. 2 D), demonstrating that the susceptibility of *Ripk1^{kd}* mice is not the result of developmental defects.

To test whether RIPK1 kinase activity promotes apoptosis in vivo during oral *Yp* infection, MLN sections were stained for bacteria and CC3. In WT MLNs, *Yp* was found primarily within lesions that showed concomitant CC3 immunostaining (Fig. 2 E). In contrast, *Ripk1^{kd}* MLNs showed areas of bacterial staining without accompanying apoptosis. Notably, bacterial colonies found in WT MLNs were primarily contained within discrete pyogranulomas, characterized by central cores of cell debris surrounded by dense cuffs of neutrophils and epithelioid macrophages (Fig. 2 F; and Fig. S1, B and C). In contrast, *Ripk1^{kd}* MLNs lacked discrete pyogranulomas, and bacterial colonies were widely dispersed throughout areas of confluent inflammation and necrosis, as well as within and bordering the subcapsular sinuses (Fig. 2 F and Fig. S1 C). Furthermore, MLNs from *Yp*-infected *Ripk1^{kd}* mice had significantly increased tissue destruction

and effacement when compared with WT mice (Fig. 2 G and Fig. S1 B). Histological analysis of splenic sections demonstrated increased bacterial colonies in *Ripk1^{kd}* mice, consistent with the observed increase in bacterial burdens at this site (Fig. S1 D). The findings of fewer discrete pyogranulomas and widespread dispersion of bacteria within the MLN of *Ripk1^{kd}* mice indicate a defect in local containment of bacteria that may facilitate dissemination to distant sites. Interestingly, in WT mice, *Yp* disseminates to hepatosplenic sites from a replicating pool of bacteria within the intestinal lumen (Barnes et al., 2006). RIPK1 kinase-induced apoptosis may therefore provide an important barrier for dissemination via the regional lymphoid route.

RIPK1 kinase-dependent apoptosis in response to *Yersinia* is triggered by YopJ-mediated blockade of NF- κ B and MAPK signaling (Boland and Cornelis, 1998; Ruckdeschel et al., 1998; Palmer et al., 1999). Intriguingly, *Ripk1^{kd}* mice infected with YopJ-deficient bacteria (Δ YopJ) showed significantly reduced histological evidence of tissue architecture effacement, and exhibited increased granuloma formation, increased survival, and improved control of bacterial burdens (Fig. 2, G–I; and Fig. S1 E) when compared with *Yp*-infected *Ripk1^{kd}* mice. Altogether, these data demonstrate that RIPK1 kinase activity is a key regulator of effector-triggered immunity in response to bacterial disruption of cell-intrinsic innate inflammatory responses.

Hematopoietic RIPK1 kinase activity is required for control of bacterial infection and in vivo cytokine production

Yp has a tropism for lymphoid tissues and preferentially targets innate immune cells (Balada-Llasat and Mecsas, 2006; Durand et al., 2010). To test the role of hematopoietic RIPK1 kinase activity in the control of *Yersinia* infection, we infected BM chimeric mice containing a congenically marked WT or *Ripk1^{kd}* hematopoietic compartment (Fig. 3 A). Similar to full *Ripk1^{kd}* mice, *Ripk1^{kd}* BM chimeras had increased bacterial burdens in both the spleen and liver, but not MLNs, when compared with WT BM chimeras (Fig. 3 B). Surprisingly, although the composition, number of immune cells in MLNs, and chimerism were equivalent between WT and *Ripk1^{kd}* BM chimeras (Fig. 3, C and D; and Fig. S2, A and B), we observed a defect in both the frequency and number of *Ripk1^{kd}* IL-12p40-producing monocytes and TNF-producing neutrophils, whereas IL-6 expression was equivalent (Fig. 3, E–G; and Fig. S2, C–E). Overall, these results demonstrate that hematopoietic RIPK1 kinase activity promotes induction of specific inflammatory cytokine responses during in vivo *Yersinia* infection.

To test whether RIPK1 kinase activity in nonhematopoietic or radioresistant cells also provides protection against *Yp*, we reconstituted WT or *Ripk1^{kd}* host mice with congenically marked WT BM (Fig. 3 H). Transfer of WT BM to *Ripk1^{kd}* mice restored the ability of *Ripk1^{kd}* hosts to control splenic bacterial burdens after oral *Yersinia* infection (Fig. 3 I). Interestingly, these mice still had increased bacte-

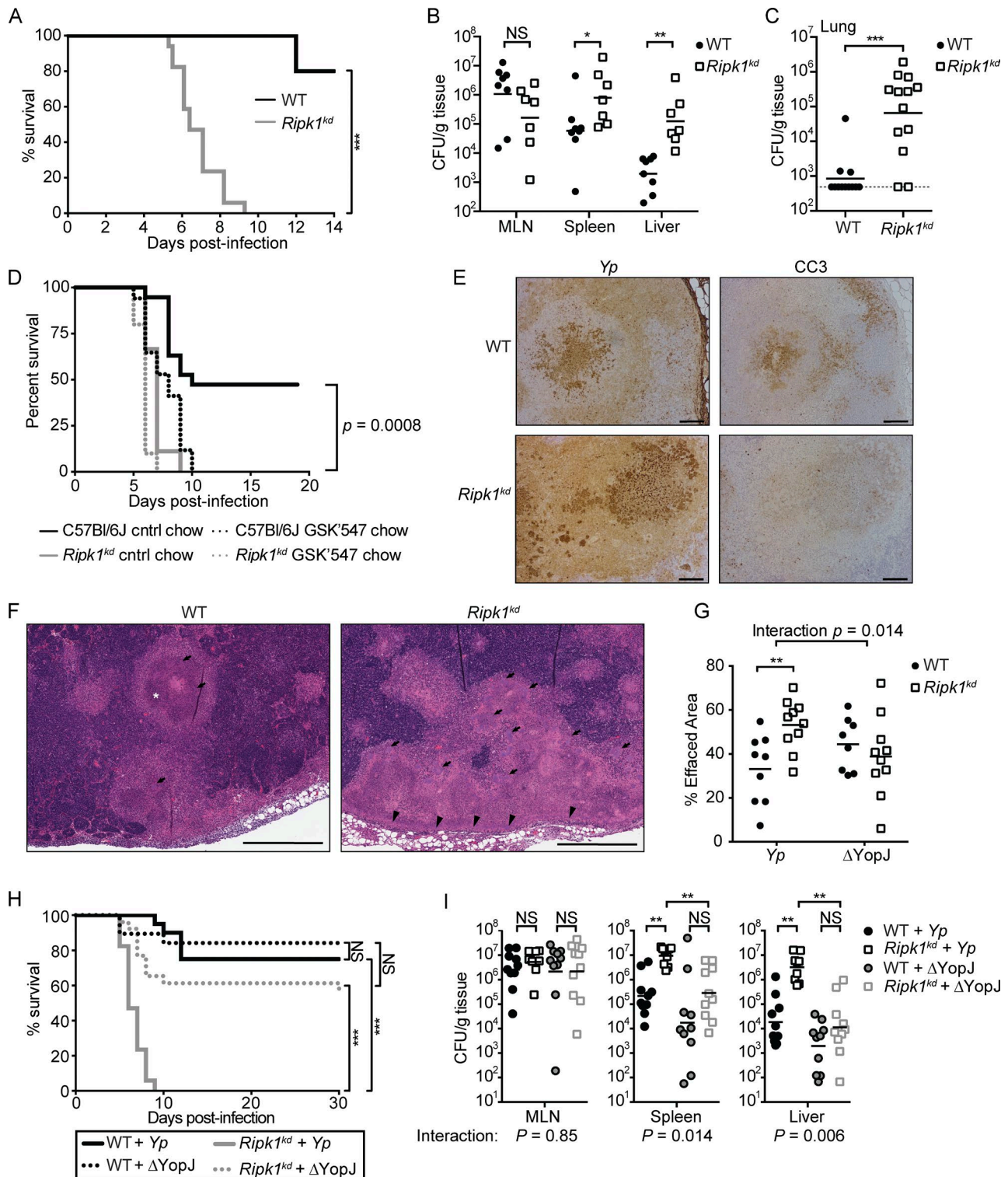


Figure 2. **RIPK1 kinase activity protects against in vivo *Yersinia* infection.** (A) Survival of WT and *Ripk1^{kd}* mice infected with 3×10^8 CFUs *Y. pseudotuberculosis* (*Yp*) by oral gavage (total $n = 10$ for WT and 17 for *Ripk1^{kd}*). (B and C) Bacterial burdens were quantified on day 5 postinfection as in A. Solid line represents the geometric mean. Dotted line represents the limit of detection in the lung. Data are representative of more than four independent experiments in A and B and three independent experiments in C. (D) Survival of mice provided with control or GSK'547 chow before being infected as in A (total $n = 10$ –19 mice per condition). (E–G) MLNs from WT and *Ripk1^{kd}* mice were harvested 5 d postinfection, as in A. (E) Parallel sections were stained by immunohistochemistry with antibodies against *Yp* or CC3. Bars, 100 μ m. (F) H&E-stained sections show WT MLNs with fewer bacterial colonies (arrows),

rial burdens in the liver compared with WT hosts, suggesting that RIPK1 kinase activity in nonhematopoietic or radio-resistant cell populations may also contribute to host protection against *Yp* infection in the liver.

Apoptotic cells associated with bacterial PAMPs can prime inflammatory T cell responses, (Torchinsky et al., 2009; Campisi et al., 2016). However, at 5 d postinfection, we observed only a small population of *Yp*-specific MLN T cells producing IFN- γ , TNF, or IL-17A (Fig. S3, A and C). We observed a small but statistically significant difference between WT and *Ripk1^{kd}* YopE₆₆₋₇₇-specific CD8⁺ T cell responses (Fig. S3, B and D), suggesting that RIPK1 kinase activity could potentially contribute to early priming of *Yp*-specific CD8⁺ T cell responses. Nevertheless, the acute and early sensitivity of *Ripk1^{kd}* mice to *Yp* infection suggested that differences in adaptive responses are unlikely to play a significant role in RIPK1-dependent control of *Yp* at this timepoint and that RIPK1 kinase activity promotes an innate immune response to infection.

RIPK1 regulates cytokine production in vivo via a cell-extrinsic mechanism

RIPK1 kinase activity is required for both caspase-8-dependent apoptosis and RIPK3-dependent necroptosis (Kelliher et al., 1998; Holler et al., 2000; Degterev et al., 2008; Ofengeim and Yuan, 2013; Silke et al., 2015). However, *Ripk3^{-/-}* BMDMs or B6 BMDMs treated with the RIPK3 inhibitor GSK'872 have WT levels of cell death after *Yersinia* infection (Philip et al., 2014; Weng et al., 2014; Peterson et al., 2016). Furthermore, BM chimeric mice with a *Ripk3^{-/-}* hematopoietic compartment have no defect in early control of *Yp* infection (Philip et al., 2014). Consistently, *Ripk3^{-/-}* and WT mice had equivalent bacterial burdens and innate cell cytokine production on day 5 postinfection (Fig. 4 A and Fig. S3 E), indicating that RIPK1 controls *Yersinia* infection independently of RIPK3.

RIPK1 kinase activity does not promote cell-intrinsic responses in the absence of necroptosis-inducing stimuli (Ting et al., 1996; Lee et al., 2004; Berger et al., 2014; Newton et al., 2014; Philip et al., 2014; Najjar et al., 2016), consistent with our observations that RIPK1 kinase activity is not required for cell-intrinsic cytokine production by BMDMs (Fig. 1, D and E). The reduced production of cytokines in vivo by *Ripk1^{kd}* monocytes and neutrophils (Fig. 3, E and F) therefore suggests that RIPK1 kinase-dependent apoptosis

provides a cell-extrinsic signal that enables cytokine production by neighboring cells. Alternatively, RIPK1 kinase activity could play a cell-type-specific role in vivo as an intrinsic regulator of cytokine production. To distinguish between these possibilities, we generated mixed BM chimeras using congenically marked WT and *Ripk1^{kd}* BM (Fig. 4 B and Fig. S3 F). Notably, the ability of *Ripk1^{kd}* neutrophils and monocyte to produce TNF or IL-12p40 was restored to WT levels in a mixed BM chimera setting and significantly elevated when compared with *Ripk1^{kd}* chimeras, whereas both sets of congenically marked WT cells produced equivalent levels of TNF and IL-12 (Fig. 4 C). These data demonstrate that the presence of WT cells restores the ability of *Ripk1^{kd}* innate immune cells to produce inflammatory cytokines in the setting of *Yp* infection. Control of bacterial tissue burdens was also restored in the mixed BM chimeras (Fig. 4 D). Collectively, these studies implicate RIPK1-dependent cell death as an important regulator of antibacterial immune defense. This work also provides the first evidence that RIPK1 kinase-induced apoptosis promotes an effector-triggered innate response that overcomes pathogen-driven blockade of inflammatory cytokine production (Fig. 4 E).

Concluding remarks

Microbial pathogens use diverse mechanisms to inhibit innate immune signaling pathways and replicate within their hosts. However, inhibition of cellular signaling pathways can also result in the induction of host cell death, a response that is evolutionarily conserved in eukaryotes (Orth et al., 2000; Mukherjee et al., 2007; Cheong et al., 2014). Here, we show that apoptotic cell death can serve as an important immunogenic signal during bacterial infection and provides a mechanism to induce inflammation despite blockade of cell-intrinsic signaling by pathogens.

YopJ-dependent blockade of TAK1 and IKK signaling during the early stages of infection can promote bacterial virulence and intestinal epithelial breakdown (Monack et al., 1998; Meinzer et al., 2012). Nonetheless, we find here that this pathogen virulence activity elicits a RIPK1-dependent apoptosis that functions as an effector-triggered immune response to promote control of bacterial burdens and innate cytokine production in vivo. This suggests an evolutionary tradeoff between the effects of YopJ and the consequent host apoptotic response; although the ancestral function of YopJ and YopJ-related proteins is to suppress cell-intrinsic

often contained within well-circumscribed pyogranulomas (asterisks). Bacterial colonies in *Ripk1^{kd}* MLNs are dispersed throughout areas of less discrete necrotizing inflammation, including in the space adjacent to the subcapsular sinus (arrowheads). Bars, 500 μ m. Images in E and F are representative of two independent experiments ($n = 9-10$ mice per group). (G) Tissue destruction and effacement of MLNs from *Yp*- and Δ YopJ-infected mice, quantified from samples stained as in F and outlined as in Fig. S1 B. Line represents the mean (total $n = 8-10$ mice per group). (H) Survival of WT and *Ripk1^{kd}* mice infected with 3×10^8 CFUs of either *Yp* or Δ YopJ by oral gavage (total $n = 18-26$ mice per condition). (I) Bacterial burdens from mice infected as in H were measured on day 5 postinfection. Data pooled from two independent experiments ($n = 8-10$ mice per group). Statistical significance in differences between bacterial burdens in B, C, and I was determined by Mann-Whitney *U* test and between percent effaced area in G by Student's *t* test. The interaction between mouse genotype and bacterial infection in G and I was tested by two-way analysis of variance. Survival data in A, D, and H were pooled from two independent experiments and statistical significance determined by log-rank test. *, $P < 0.05$; **, $P < 0.01$; ***, $P < 0.001$; NS, not significant.

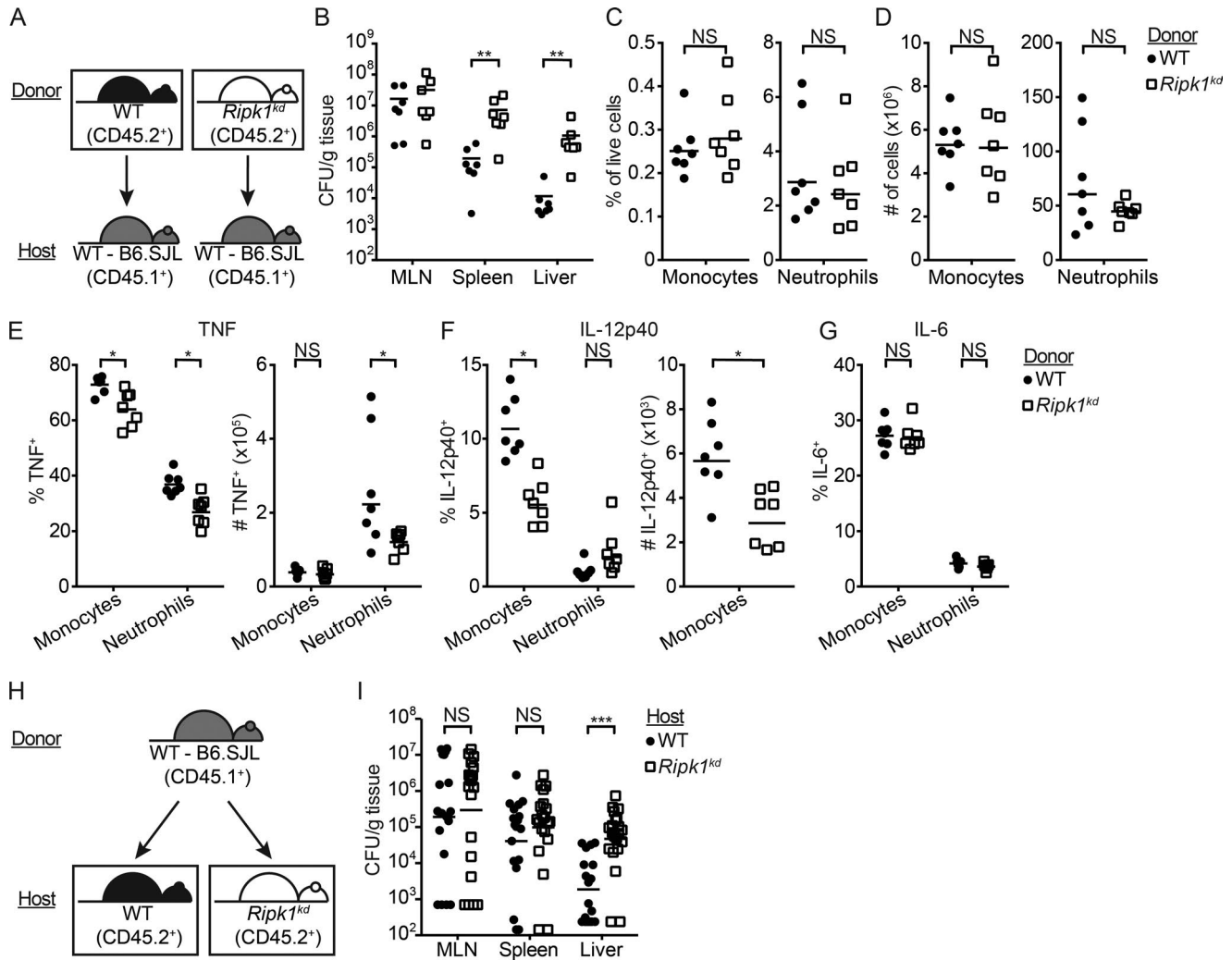


Figure 3. Hematopoietic RIPK1 kinase activity is required for optimal control of bacterial infection and in vivo cytokine production. (A) BM chimeras were generated by reconstituting lethally irradiated congenic hosts with BM from either WT or *Ripk1*^{kd} mice. (B) BM chimeric mice were infected with $1-2 \times 10^8$ CFUs *Y. pseudotuberculosis*, and tissue bacterial burdens were measured on day 5 postinfection. Line represents the geometric mean. (C and D) Frequency of live cells and the number of inflammatory monocytes (CD11b^{hi}Ly6C^{hi}Ly6G⁻) and neutrophils (CD11b^{hi}Ly6G⁺) in the MLNs of infected mice were measured by flow cytometry on day 5 postinfection. (E-G) Cytokine expression by innate immune cell populations isolated from MLNs was measured by flow cytometry on day 5 postinfection. Line represents the mean. Data in B-G are representative of three independent experiments ($n = 7$ mice per group). (H) Chimeric mice were generated by reconstituting lethally irradiated WT or *Ripk1*^{kd} hosts with WT congenic BM. (I) BM chimeric mice were infected as in A, and bacterial burdens measured on day 5 postinfection. Line represents the geometric mean. Data were pooled from two independent experiments, each with similar results ($n = 18-21$ mice per group). Statistical significance in B and I was determined by Mann-Whitney *U* test and in C-G by Student's *t* test. *, $P < 0.05$; **, $P < 0.01$; ***, $P < 0.001$; NS, not significant.

host signaling, the apoptotic response serves as a host defense mechanism that bypasses the pathogen-driven blockade of immune signaling.

The contribution of RIPK1 kinase to innate cytokine production during *Yersinia* infection is mediated by a cell-extrinsic signal, consistent with a model in which cell death allows for the propagation of an inflammatory stimulus to neighboring cells (Fig. 4 E). In contrast to pyroptosis or necrosis, apoptosis has historically been viewed as a primarily immunosuppressive form of cell death (Green et al., 2009;

Blander, 2014). Previous studies on the regulation of cell death-induced inflammation by RIPK1 kinase activity have, therefore, focused primarily on RIPK3-dependent necroptosis (Berger et al., 2014; Newton et al., 2014, 2016; Polykratis et al., 2014; Silke et al., 2015; Weinlich et al., 2017). RIPK1 kinase activity can also promote cytokine expression under necroptosis-inducing conditions or during caspase inhibition, even in the absence of cell death (Najjar et al., 2016). However, this effect of RIPK1 kinase activity is both cell-intrinsic and dependent on RIPK3 (Najjar et al., 2016). Another re-

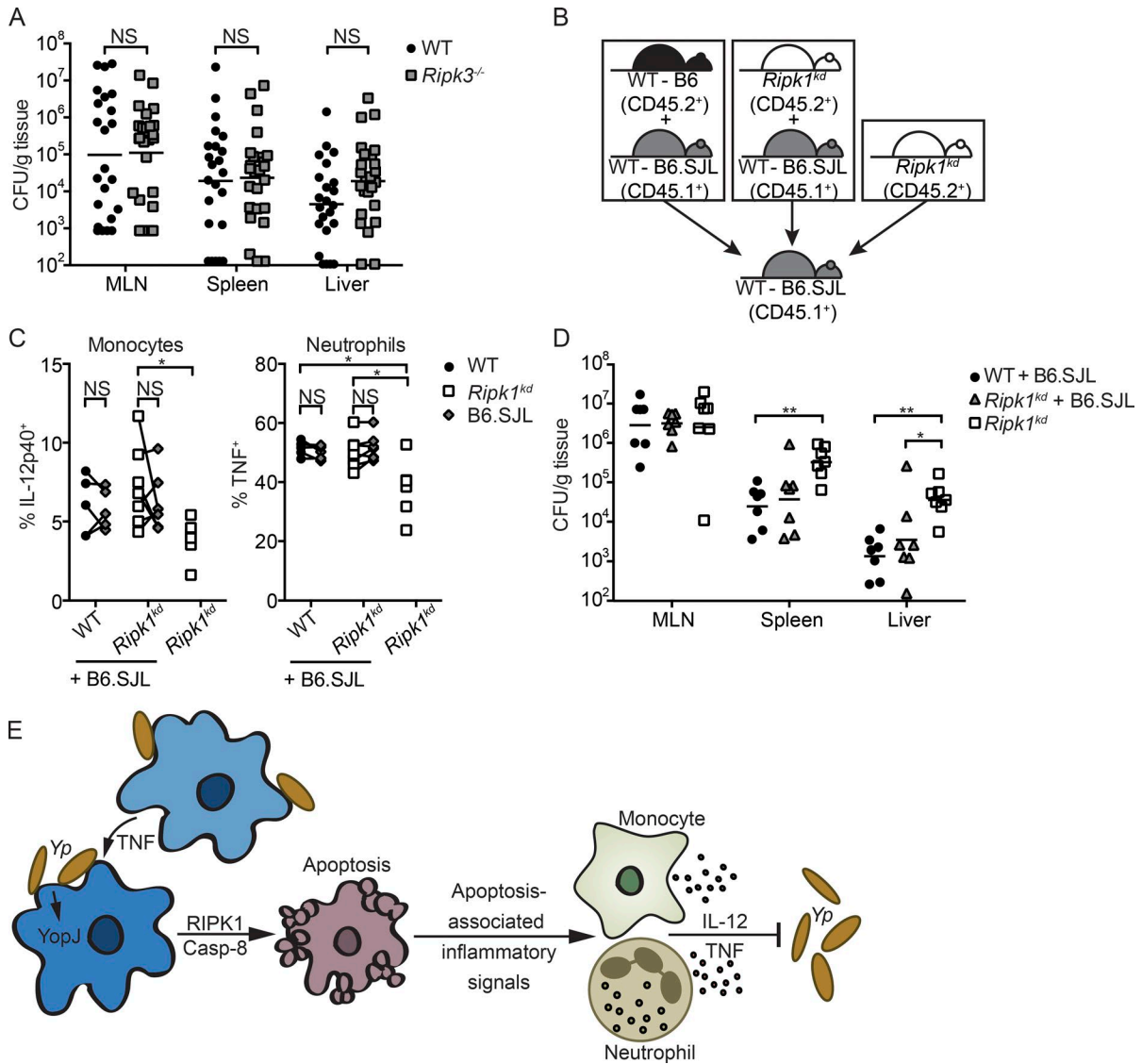


Figure 4. RIPK1 is a cell-extrinsic regulator of in vivo cytokine production. (A) WT and RIPK3-deficient mice were infected with 2×10^8 CFUs *Y. pseudotuberculosis* (*Yp*) by oral gavage and bacterial burdens measured on day 5 postinfection. Line represents the geometric mean. Data pooled from three independent experiments, each with similar results ($n = 23\text{--}25$ mice per group). (B) Mixed BM chimeras were generated by reconstituting lethally irradiated congenic hosts with a 1:1 mixture of either WT or *Ripk1^{kd}* BM (CD45.2⁺) and WT congenic B6.SJL BM (CD45.1⁺). (C) Chimeric mice were infected with 2×10^8 CFUs *Yp*, and cytokine expression on day 5 postinfection was measured by flow cytometry. Congenic labeling of donor cells allowed for comparison within individual mice (paired *t* test) in addition to comparison across experimental groups (unpaired *t* test). Lines connect congenic cell populations within individual mice. (D) Bacterial burdens were measured on day 5 postinfection of mixed BM chimeras. Data in C and D are representative of three independent experiments ($n = 7$ mice per group). Statistical significance in bacterial burdens in A and D was determined by Mann-Whitney *U* test. *, $P < 0.05$; **, $P < 0.01$; NS, not significant. (E) Model of YopJ-mediated inhibition, RIPK1-dependent apoptosis, and the induction of host-protective antibacterial inflammatory responses.

cent study suggests that caspase-8-dependent apoptosis and RIPK3-dependent necrosis can act cooperatively to promote inflammatory responses against viral infection (Daley-Bauer et al., 2017). Here, we provide evidence that RIPK1 kinase-induced apoptosis has a cell-extrinsic role in host survival and innate antimicrobial immune defense that is independent of RIPK3 and necroptosis.

In summary, our data demonstrate that RIPK1 kinase-dependent cell death has an essential role in promoting host innate immunity during bacterial infection. Selective disruption of pathogen-induced cell death, while leaving other pathogen-responsive immune signaling pathways intact, enabled us for the first time to distinguish the effects of pathogen virulence factors on inhibition of host cell signaling

from pathogen-induced apoptosis. Collectively, these studies provide new insight into the innate host defense function of RIPK1 kinase activity and establish RIPK1 as a mediator of effector-triggered immunity. Further studies of the signals released during this pathway of apoptosis to generate inflammatory responses will further define the relationships among cell death, inflammation, and immunity and may provide novel targets for therapeutic intervention.

MATERIALS AND METHODS

Cell culture and in vitro infections

BMDMs were grown as described previously (Philip et al., 2014) in non-tissue culture (non-TC) –treated Petri dishes in a 37°C humidified incubator in DMEM supplemented with 10% FBS, Hepes, sodium pyruvate (complete DMEM), and 30% L929 supernatant for 7–9 d. 16–20 h before infection, cells were harvested with cold PBS and replated into TC-treated (lactate dehydrogenase [LDH], Western blot) or non-TC-treated (flow cytometry) plates in complete DMEM containing 10% L929 supernatant. Cells were treated with 60 μ M Nec-1 (Calbiochem) 1 h before infection where indicated. For TLR ligand stimulation, cells were treated with 1 μ g/ml Pam3CK, 50 μ g/ml poly(I:C), 1 μ g/ml CpG, or 50 ng/ml LPS. For bacterial infections, WT *Yersinia* strain 32777 (*Yp*) or isogenic YopJ-deficient mutant (Δ YopJ; Zhang and Bliska, 2010) was grown overnight with aeration in 2 \times YT broth at 26°C. Bacteria were diluted into inducing media (2 \times YT containing 20 mM sodium oxalate and 20 mM MgCl₂) and grown with aeration for 1 h at 26°C followed by 2 h at 37°C. Bacteria were washed three times with warm complete DMEM, added to BMDM cultures at a multiplicity of infection of 20:1, and spun onto cells at 1,000 rpm for 5 min. Cells were incubated at 37°C, and 100 μ g/ml gentamicin was added 1 h after infection.

In vitro cell death assays

For LDH release, BMDMs were plated into TC-treated plates in complete DMEM containing 10% L929 supernatant. LDH release was measured from cell supernatants of infected BMDMs and quantified using the Cytotox96 Assay kit (Promega) according to manufacturer's instruction. Flow cytometry measurement of CC3 was performed by harvesting infected BMDMs with cold PBS containing 2% EDTA and staining with the Zombie Yellow Fixable Viability kit (BioLegend) before fixation and permeabilization (BD Cytofix/Cytoperm kit). Cells were then stained for CC3 (9661; Cell Signaling), followed by secondary anti-rabbit Alexa Fluor 488. Samples were run on an LSRFortessa and analyzed using FlowJo Tree Star software.

Western blotting and ELISA

Cell lysates were harvested from cells infected in TC-treated plates with lysis buffer and run on 4–12% NuPAGE gels (Invitrogen). Proteins were transferred to PVDF membrane (Millipore) and blotted with rat anti-mouse caspase-8 (1G12;

Enzo Life Sciences), rabbit anti-caspase-3 (9662; Cell Signaling) and β -actin (Sigma), followed by HRP-conjugated secondary antibodies. Cytokine release was measured by ELISA on cell supernatants using capture and detection antibodies against TNF (BioLegend), IL-6 (BD), and IL-12p40 (BD).

Mice

C57BL/6J control (CD45.2) and C57BL/6.SJL (CD45.1) mice were obtained from The Jackson Laboratory. Ripk1 kinase-dead (*Ripk1^{kd}*) mice with K45A mutation have been previously described (Berger et al., 2014). *Ripk3^{-/-}* mice were provided by V.M. Dixit (Genentech). Age- and sex-matched 8–12-wk-old mice were used for all experiments. For generation of BM chimeric mice, 8–10-wk-old congenically marked (CD45.2 or CD45.1) mice were lethally irradiated with 1,100 rads (either a single dose or split into two doses 24 h apart). $3\text{--}5 \times 10^6$ congenic BM cells were transferred i.v. by retro-orbital injection. Chimeras were allowed to reconstitute for 9–12 wk. All animal studies were performed under Institutional Animal Care and Use Committee-approved protocols and in accordance with the guidelines of the Institutional Animal Care and Use Committee of the University of Pennsylvania.

Animal infections

For intravenous infections, mice were infected retro-orbitally with 2×10^8 CFUs WT *Yp* (32777) or an isogenic avirulent strain lacking an essential virulence plasmid (*Yp^P*). Before injection, bacteria were cultured under inducing conditions, as for in vitro infections. 4 h after infection, spleens were harvested and promptly isolated for flow cytometry staining of CC3, along with cell type-specific surface markers. For oral infection, mice were fasted for 12–16 h and inoculated by intragastric gavage with $1\text{--}3 \times 10^8$ CFUs WT (32777) or isogenic YopJ-deficient (Δ YopJ) *Yp* from overnight culture and washed with PBS. For intraperitoneal infections, mice were injected with 2×10^4 CFUs. Mice were euthanized, and tissues were collected and weighed in 1 ml sterile PBS, bead homogenized (MP Biomedical), and plated at 10-fold dilutions on LB plates containing irgasan to determine bacterial burdens (CFU/g tissue). For oral *Yp* infection of animals treated with RIPK1 kinase inhibitor, C57BL6/J mice were placed on a diet of irradiated Purina 5001 control chow or chow containing RIPK1 inhibitor GSK3540547A (GSK'547 chow, provided by GSK) 2 d before infection and allowed to eat ad libitum for the duration of the experiment.

Histopathology

MLNs and spleens were fixed in 10% neutral buffered formalin, paraffin embedded, sectioned, and stained with hematoxylin and eosin (H&E). For immunohistochemical staining, sections were stained with rabbit anti-*Yp* antibody (J. Bliska, Stony Brook University, Stony Brook, NY) or rabbit anti-CC3 (1:500, 9679; CST) and SignalStain IHC detection reagent (12692; CST). Slides were imaged on an Olym-

pus BX53 microscope with an Olympus DP25 camera or a Nikon Eclipse TE2000-U microscope with a Nikon DS-Ri1 camera. For analysis of tissue effacement, H&E-stained MLN sections were imaged on an Aperio CS-O scanner, and areas were traced manually and measured by a blinded board-certified pathologist using ImageJ software.

Flow cytometry

MLN cells were isolated by passing through a 100- μ M cell strainer. To measure cytokine expression by innate immune cells (neutrophils, monocytes, and DCs), 3–5 $\times 10^6$ isolated cells were plated in a 96-well plate and cultured for 5 h in the presence of brefeldin A (Sigma) and monensin (BD) in a 37°C humidified incubator in complete DMEM containing penicillin–streptomycin and 2-mercaptoethanol. For stimulation and intracellular cytokine staining of T cells, 2–3 $\times 10^6$ isolated cells were plated and cultured for 2 h in the presence of either heat-killed *Yp* (HKYp) or YopE_{69–77} peptide and for 3 h in the presence of brefeldin A and monensin. Cells were washed with PBS, stained for viability (Zombie Yellow; BioLegend), and then stained with the following antibodies: Ly6G (1A-8; BioLegend), IL-6 (MP5-20F3; BioLegend), CD45.1 (A20; BD Biosciences), CD45.2 (104; BD Biosciences), MHCII (M5/114; BD Biosciences), CD11b (M1/70.15; ThermoFisher), Ly6C (HK1.4; eBioscience), CD11c (N418; eBioscience), TNF (MP6-XT22; eBioscience), IL-12p40 (C17.8; eBioscience), and H-2K(b) YopE_{69–77} Alexa 488-labeled tetramer (NIH Tetramer Core Facility). For innate cell analysis, singlet, live cells were gated to identify neutrophils (CD11b^{hi}Ly6G⁺), inflammatory monocytes (CD11b^{hi}Ly6C^{hi}Ly6G⁻), or DCs (CD11c⁺MHCII^{hi}) as shown in Fig. S2. Gating for cytokine-positive cells was based on fluorescence-minus-one and naive control samples. For T cell analysis, cells were gated for CD4⁺, and CD8⁺ T cells were identified from B220⁻CD11b⁻CD3⁺ cells. For BM chimera experiments, CD45.1/CD45.2 staining was used to distinguish between host and donor cell origin. Surface staining was performed in FACS buffer (PBS with 1% BSA, 2 mM EDTA) and sample fixation and permeabilization performed before intracellular staining according to manufacturer's instructions (BD Cytofix/Cytoperm kit). Samples were run on an LSRFortessa and analyzed using FlowJo Tree Star software.

Statistical analysis

Statistical analysis was performed using Prism software by GraphPad. Unless otherwise specified, comparisons between percentages, protein concentrations, and numbers of cells between groups was performed by unpaired *t* test. Comparisons between bacterial burdens were performed by Mann–Whitney *U* test and survival curves by log-rank (Mantel–Cox) test.

Online supplemental material

Fig. S1 shows spleen CFUs in B6 and *Ripk1*^{kd} mice after intraperitoneal injection of bacteria, and histopathology (H&E) and immunohistochemistry staining for *Yersinia* in

infected MLN and spleen sections. Fig. S2 shows the percent chimerism in BM chimeric mice after transplant of B6 or *Ripk1*kd BM into irradiated congenic recipient hosts and the gating strategies used to characterize specific immune cell populations. Fig. S3 shows adaptive immune responses in B6 and *Ripk1*^{kd} mice and intracellular cytokine production in *Ripk3*^{-/-} neutrophils and monocytes from MLN cells.

ACKNOWLEDGMENTS

Tetramer reagents were provided by the National Institutes of Health Core Tetramer Facility, and anti-*Yersinia* antibodies were a gift from James Bliska. We would like to thank Sunny Shin for critical reading and scientific discussion.

This work was supported by the National Institutes of Health (grants AI103062, AI128530, and AI109267), a Burroughs Wellcome Fund Investigator in the Pathogenesis of Infectious Disease Award (to I.E. Brodsky), the Training Program in Rheumatic Diseases (grant T32-AR007442 to L.W. Peterson), and a National Science Foundation Graduate Research Fellowship Award (to A. DeLaney).

S.B. Berger, P.J. Gough, and J. Bertin are employees of GlaxoSmithKline. The authors declare no additional competing financial interests.

Author contributions: L.W. Peterson and N.H. Philip conceived the study, designed and performed experiments, and analyzed data. A. DeLaney and M.A. Wynosky-Dolfi designed and performed experiments and analyzed data. K. Asklof, R. Choa, E. Bjanas, and B. Hu performed experiments. F. Gray and E.L. Buza performed blinded histopathology analysis. C.P. Dillon, D.R. Green, S.B. Berger, P.J. Gough, and J. Bertin provided invaluable mice and reagents. I.E. Brodsky conceived and directed the study and wrote the manuscript with L.W. Peterson.

Submitted: 22 February 2017

Revised: 19 July 2017

Accepted: 17 August 2017

REFERENCES

- Balada-Llasat, J.-M., and J. Mecsas. 2006. *Yersinia* has a tropism for B and T cell zones of lymph nodes that is independent of the type III secretion system. *PLoS Pathog.* 2:e86. <http://dx.doi.org/10.1371/journal.ppat.0020086>
- Barnes, P.D., M.A. Bergman, J. Mecsas, and R.R. Isberg. 2006. *Yersinia pseudotuberculosis* disseminates directly from a replicating bacterial pool in the intestine. *J. Exp. Med.* 203:1591–1601. <http://dx.doi.org/10.1084/jem.20060905>
- Berger, S.B., V. Kasparcova, S. Hoffman, B. Swift, L. Dare, M. Schaeffer, C. Capriotti, M. Cook, J. Finger, A. Hughes-Earle, et al. 2014. Cutting Edge: RIP1 kinase activity is dispensable for normal development but is a key regulator of inflammation in SHARPIN-deficient mice. *J. Immunol.* 192:5476–5480. <http://dx.doi.org/10.4049/jimmunol.1400499>
- Blander, J.M. 2014. A long-awaited merger of the pathways mediating host defence and programmed cell death. *Nat. Rev. Immunol.* 14:601–618. <http://dx.doi.org/10.1038/nri3720>
- Boland, A., and G.R. Cornelis. 1998. Role of YopP in suppression of tumor necrosis factor alpha release by macrophages during *Yersinia* infection. *Infect. Immun.* 66:1878–1884.
- Brodsky, I.E., and R. Medzhitov. 2009. Targeting of immune signalling networks by bacterial pathogens. *Nat. Cell Biol.* 11:521–526. <http://dx.doi.org/10.1038/ncb0509-521>
- Campisi, L., G. Barbet, Y. Ding, E. Esplugues, R.A. Flavell, and J.M. Blander. 2016. Apoptosis in response to microbial infection induces autoreactive TH17 cells. *Nat. Immunol.* 17:1084–1092. <http://dx.doi.org/10.1038/ni.3512>

